



# Enhanced metamorphic CO<sub>2</sub> release on the Proterozoic Earth

E. M. Stewart<sup>a,1</sup> and Donald E. Penman<sup>b</sup>

Edited by David C. Catling, University of Washington, Seattle, WA; received January 29, 2024; accepted August 12, 2024 by Editorial Board Member Michael Manga

Rock metamorphism releases substantial CO<sub>2</sub> over geologic timescales (>1 My), potentially driving long-term planetary climate trends. The nature of carbonate sediments and crustal thermal regimes exert a strong control on the efficiency of metamorphic CO<sub>2</sub> release; thus, it is likely that metamorphic CO<sub>2</sub> degassing has not been constant throughout time. The Proterozoic Earth was characterized by a high proportion of dolomite-bearing mixed carbonate-silicate rocks and hotter crustal regimes, both of which would be expected to enhance metamorphic decarbonation. Thermodynamic phase equilibria modeling predicts that the metamorphic carbon flux was likely ~1.7 times greater in the Mesoproterozoic Era compared to the modern Earth. Analytical and numerical approaches (the carbon cycle model PreCOSCIOUS) are used to estimate the impact this would have on Proterozoic carbon cycling and global atmospheric compositions. This enhanced metamorphic CO<sub>2</sub> release alone could increase pCO<sub>2</sub> by a factor of four or more when compared to modern degassing rates, contributing to a stronger greenhouse effect and warmer global temperatures during the expansion of life on the early Earth.

Proterozoic | metamorphism | carbon cycle

Metamorphic CO<sub>2</sub> degassing is a significant flux in the geologic carbon cycle with the potential to trigger global environmental change and drive the long-term evolution of the deep Earth, yet characterization of this important carbon flux prior to the Cambrian period is almost nonexistent. Nevertheless, there is reason to suspect that metamorphic CO<sub>2</sub> devolatilization was substantially higher on the earlier Earth. For one, changes in the nature of sedimentary carbonate burial have altered the distribution of carbonate in sediments which are available for metamorphism (e.g., refs. 1 and 2). In addition, hotter crustal thermal regimes prior to the Cambrian period (e.g., refs. 3 and 4) could also enhance metamorphic CO<sub>2</sub> loss.

On the modern Earth, metamorphic CO<sub>2</sub> release is on the order of ~1 to 5 Tmol CO<sub>2</sub> y<sup>-1</sup>, accounting for a significant fraction of solid Earth degassing. Though there are large uncertainties (from ~5 to ~80%), median estimates rank metamorphic degassing as ~40% of total solid Earth CO<sub>2</sub> release today (5–14). A larger Precambrian metamorphic carbon flux would have profound implications for the whole Earth system—contributing to higher atmospheric CO<sub>2</sub> concentrations and warmer climates—unless dampened or balanced by adjustment of other carbon fluxes. Thus, it is crucial to understand the factors which controlled metamorphic decarbonation on the early Earth.

Metamorphic decarbonation reactions usually occur via the reaction of silicate and carbonate minerals as often represented by the archetypical reaction:

$$CaCO_{3(calcite)} + SiO_{2(quartz)} \rightarrow CaSiO_{3(wollastonite)} + CO_{2(fluid)},$$
 [1]

where the minerals calcite and quartz react to form a new mineral, wollastonite, and release CO<sub>2</sub> (15, 16). While this specific reaction is relatively rare on Earth, it represents two important factors shared by almost all metamorphic decarbonation reactions: 1) both carbonate minerals (e.g., calcite) and silicate minerals (e.g., quartz) must be present for the reaction to go forward and 2) the reaction is driven forward at higher temperatures, thus hotter rocks can release more CO<sub>2</sub>.

In fact, the ratio of carbonate to silicate material in a rock is a strong predictor of the degree of carbon loss it will experience. A rock with a high ratio of carbonate to silicate will exhaust all silicate reactant with much of the initial carbon still trapped in solid form. Conversely, a rock with a low carbonate to silicate ratio will be limited by carbonate availability and has the potential to degas a much higher percentage of its CO<sub>2</sub> (see ref. 17).

Dolomitic rocks can also release more CO<sub>2</sub> than metamorphism of analogous calcite-bearing sediments. This is due to the higher number of product silicate minerals which may form. Reaction 2 shows the reaction of dolomite and quartz to release CO<sub>2</sub> and create calcite and forsterite as additional products.

$$2\text{CaMg}(\text{CO}_3)_{2 \; dolomite} + \text{SiO}_{2 \; quartz} \rightarrow 2\text{CaCO}_{3 \; calcite} + \text{Mg}_2 \text{SiO}_{4 \; forsterite} + 2\text{CO}_{2 \; fluid}.$$

## **Significance**

Geologic sources of atmospheric CO<sub>2</sub> were critical to maintaining Earth's habitability during the early evolution and expansion of life. It is often assumed that higher rates of volcanic outgassing provided the greenhouse gases necessary to warm the planet when solar luminosity was low; however, we demonstrate that CO<sub>2</sub> release due to metamorphic processes may have been substantially elevated from one to two billion years ago. Carbon cycle models suggest that enhanced metamorphism alone (or in combination with differences in marine weathering processes) can explain observations of a warm planet in this mid-Proterozoic Era.

Author affiliations: aDepartment of Earth, Ocean and Atmospheric Science, Florida State University, Tallahassee, FL 32306; and <sup>b</sup>Department of Geosciences, Utah State University, Logan, UT 84322

Author contributions: E.M.S. and D.E.P. designed research; performed research; analyzed data; and wrote

The authors declare no competing interest.

This article is a PNAS Direct Submission. D.C.C. is a guest editor invited by the Editorial Board.

Copyright © 2024 the Author(s). Published by PNAS. This article is distributed under Creative Commons Attribution-NonCommercial-NoDerivatives License 4.0 (CC BY-NC-ND).

<sup>1</sup>To whom correspondence may be addressed. Email: emstewart@fsu.edu.

This article contains supporting information online at https://www.pnas.org/lookup/suppl/doi:10.1073/pnas. 2401961121/-/DCSupplemental.

Published September 23, 2024.

In addition to forsterite, reaction of dolomite and quartz may form talc, tremolite, diopside, or clinohumite (16). Calcite and quartz, on the other hand, can only react to form the mineral wollastonite at crustal P-T conditions. Many Mg-bearing silicates are stable at lower temperatures than wollastonite (e.g., talc at ~300 °C versus wollastonite at 700 °C; see ref. 16). At high temperatures, stable Mg-silicates exhibit lower cation-to-silicon ratios than wollastonite (e.g., 2:1 in forsterite versus 1:1 in wollastonite). Thus, dolomitic rocks undergo more efficient decarbonation than calcitic rocks if they are either a) silica limited and/or b) experienced peak temperatures below ~700 °C.

Given the above, this work focuses on how two broad variables have changed over billions of years: first, the nature of protolith sediments available to be metamorphosed, and second, the pressure-temperature (P-T) conditions of metamorphism itself. Here, we show that these intertwined variables may combine to dramatically increase metamorphic CO<sub>2</sub> degassing and atmospheric CO<sub>2</sub> concentrations on the earlier Earth, making metamorphism a critical component of our planet's early habitability.

**Exploring Metamorphic Decarbonation Efficiency.** Thermodynamic modeling of rock metamorphism can be used to explore the influence that protolith bulk composition and P-T conditions exert on decarbonation efficiency. As an example, the degree of decarbonation is calculated for a range of bulk compositions: one endmember is a representative siliceous sediment with no carbonate material (Marianas clay composition from ref. 18) and the other endmember is a pure calcite limestone. In Fig. 1*A*, carbon loss is calculated at an arbitrary moderate temperature

and pressure of 600 °C and 0.55 GPa. At these conditions, rocks starting with <~12 weight percent calcite are able to undergo 100% decarbonation, while more calcite-rich rocks retain more of their carbon in solid form. In Fig. 1B, carbon loss for a 90% clay-10% calcite protolith is calculated along two P-T paths: a high T/P path from 310 °C and 0.2 GPa up to 600 °C and 0.55 GPa typical of Proterozoic metamorphism and a lower T/P path from 310 °C and 0.4 GPa up to 600 °C and 0.84 GPa, representing Phanerozoic Barrovian conditions (e.g., refs. 19 and 20). As expected, the rock metamorphosed along the higher T/P path releases more CO<sub>2</sub> at each temperature step. Finally, we consider decarbonation of calcite versus dolomite in Fig. 1C. Here, a carbonate + quartz system degasses CO<sub>2</sub> at lower temperatures and achieves a higher total degree of decarbonation if the carbonate mineral is dolomite. Taken together, these data suggest that higher T/P metamorphism of a predominately dolomitic and mixed carbonate-silicate sedimentary sequence would release more CO<sub>2</sub> than low T/P metamorphism of a less-mixed sequence containing an identical mass of carbon.

**Global Changes in Sedimentation and Metamorphism.** Sedimentary carbonate is dominantly (by mass) deposited in relatively pure limestones and dolostones with little to no silicate material mixed in (e.g., ref. 21). As compared to the systems in Eqs. 1 and 2, these pure carbonate rocks do not have the necessary chemical components to release CO<sub>2</sub> via decarbonation reactions at normal metamorphic conditions. While aqueous transport of, e.g., silica, into pure carbonates during metamorphism may drive

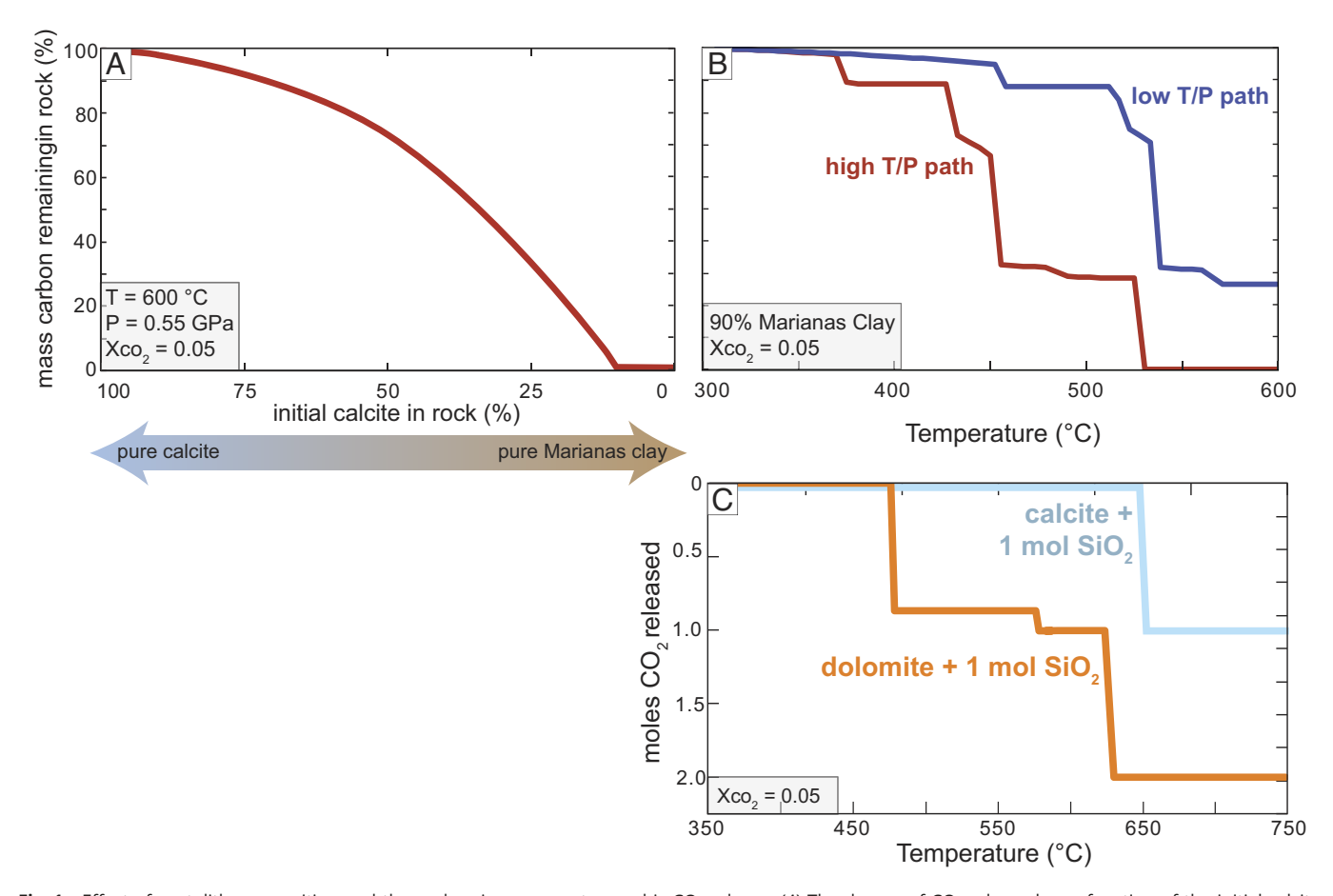


**Fig. 1.** Effect of protolith composition and thermal regimes on metamorphic CO<sub>2</sub> release. (A) The degree of CO<sub>2</sub> released as a function of the initial calcite percentage shows that rocks with <~12% calcite by weight can achieve 100% decarbonation at moderate metamorphic grade. (B) A rock on the higher T/P path typical of Precambrian metamorphism (red) begins decarbonation at lower temperatures and achieves more total carbon loss than the same rock along a lower T/P path typical of the Phanerozoic. (C) A dolomitic rock will degas more CO<sub>2</sub> than a calcitic rock along the same low T/P path shown in panel B.

decarbonation, this metasomatism is likely to affect only a small fraction of the total rock volume [~1 to 20 %; (22)].

However, the evolution of marine calcifiers around the Cambrian period had a profound effect on the nature and location of carbonate deposition (e.g., refs. 2 and 23), as documented by a rich literature on Precambrian carbonate sedimentation styles and structures (e.g., refs. 1 and 24-28). In particular, the Precambrian is characterized by a higher abundance of abiotic carbonate precipitate textures (e.g., ref. 1) and stromatolites (e.g., ref. 29). With respect to carbonate-silicate mixing, Grotzinger & James (ref. 1) note that Mesoproterozoic carbonate platforms are "muddier," with more silt and clay mixed in. The ratio of dolomite to calcite in the sedimentary record has also been thoroughly explored, with dramatically greater dolomite abundance recognized in the Archean and Proterozoic Eons, (30–33).

A large new dataset offers the opportunity to explore these observations more quantitatively. Cantine et al. (ref. 34) compiled data on carbonate-bearing sediments from 3.8 billion to 490 Mya in a database that includes observation of more than 16,000 Precambrian rocks, spanning more than 45,000 m of measured stratigraphy. Most relevant to decarbonation, each entry is flagged if it contains dolomite, "significant carbonate component in a

siliciclastic rock," or "significant siliciclastic component in a carbonate rock." Fig. 2 A and B show the distribution of rock types for each geologic era calculated from the dataset of ref. 34. A gradual increase in mixed carbonate-silicate rocks peaks in the Mesoproterozoic era, where more than 25% of the recorded section consists of these mixed rock types. Importantly, this database approach is consistent with the more qualitative observations previously made by ref. 1. In addition, the database reproduces observations of dolomitic carbonates dominating the rock record prior to the Cambrian. Thus, while there is certainly some preservation bias in these data—ref. 34 provides a more detailed discussion of possible biases and caveats in the database—we consider these two very substantial differences to represent a real change in carbonate sedimentation styles over time, consistent with the field observations made by previous authors (e.g., refs. 1 and 24).

With respect to temperature and pressure in the crust, existing analysis has already demonstrated higher metamorphic T/P conditions prior to the Cambrian (e.g., refs. 3, 4, and 35). This general cooling trend started about two billion years ago and is accompanied by spreading of P-T conditions into a bimodal distribution of hotter and colder environments. Brown & Johnson (ref. 35) report a database of 546 localities with metamorphic pressure and

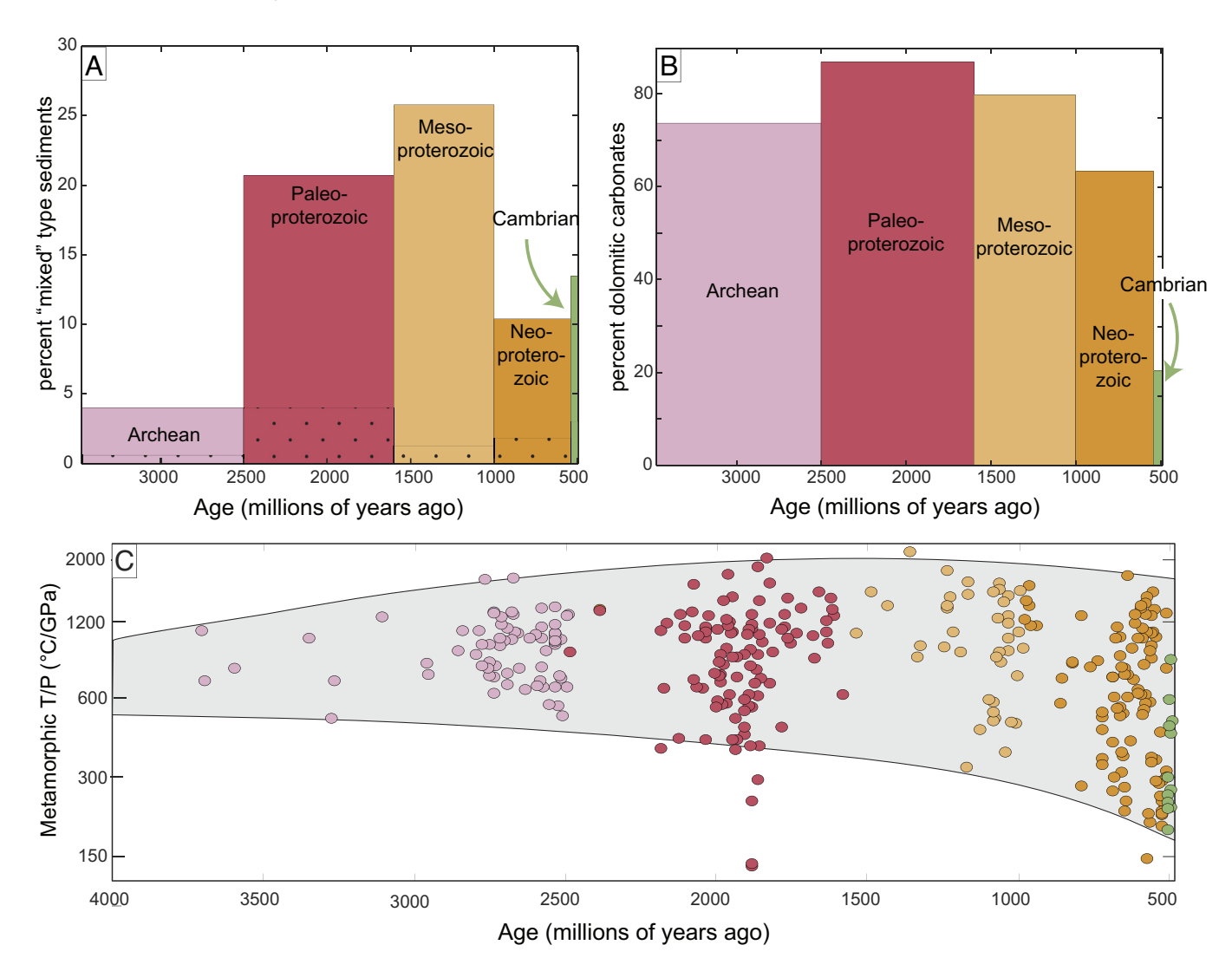


Fig. 2. Changes in carbonate sedimentation and metamorphic P-T conditions. (A and B) data from ref. 34 A shows the total proportion of mixed carbonatesilicate sediments in the rock record while dotted areas represent the contribution from rocks designated significant carbonate component in a siliciclastic rock only. (B) is the proportion of carbonate sediments which are dominantly dolomitic. (C) Modified after (4), shows the changing metamorphic P-T conditions up to and including the Cambrian period.

temperature spanning the last  $\sim$ 3.7 billion years of Earth history. Additional analysis by ref. 4 highlights the bifurcation trend and presents implications for the initiation of plate tectonics. These data are shown in Fig. 2C.

Estimating the Precambrian Metamorphic Carbon Flux.  $In \,$ order to estimate metamorphic carbon fluxes on the Precambrian Earth, thermodynamic modeling of metamorphism is applied to representative sedimentary protoliths and P-T conditions derived from ref. 34 and ref. 35, respectively. Due to the age range available in these datasets, we consider time intervals between 490 and 3500 Ma. A 10,000—iteration Monte Carlo approach is used to account for uncertainty in a variety of terms including protolith characteristics, P-T-Xco<sub>2</sub> conditions, and tectonic geometry (i.e., crustal thickness and area of metamorphism). We generate random time-bins for each iteration to avoid bias associated with binning; then, for each time interval, we calculate an average metamorphic flux as described below (*Materials and Methods* and *SI Appendix*). We calculate total solid-Earth degassing rates for each of our time bins by adding the calculated metamorphic flux to an assumed constant volcanic flux of 4 Tmol CO<sub>2</sub> y<sup>-1</sup>. In addition, the carbon isotope composition of the solid Earth degassing flux can be estimated as a weighted average of a volcanic mantle source  $(\delta^{13}C_{VPDB} = -5)$  and a heavy fractionated metamorphic source. We recognize the simplifications inherent in these calculations; however, given the consistent approach, the results can be expected to show robust patterns and relative changes between time intervals even if the absolute values carry large uncertainties.

Model inputs and results of thermodynamic modeling are shown in Fig. 3. Here and elsewhere we focus on the average model output, while 25th and 75th percentile contours are also shown. Rocks around the Archean–Proterozoic boundary at 2500 Ma undergo the lowest degree of metamorphic carbon loss, releasing an average of ~2.5 Tmol CO $_2$  per year. Mean estimated metamorphic decarbonation reaches a maximum of ~5.5 Tmol CO $_2$  per year at ~1400 Ma before falling back to ~3.5 Tmol y $^{-1}$  in the Cambrian. When added to a constant volcanic flux, this corresponds to total solid Earth outgassing increasing from ~6.5 Tmol CO $_2$  per year on the earliest Earth to ~9.5 Tmol CO $_2$  per year in the Proterozoic (i.e., an increase of ~45%). The  $\delta^{13}$ C of the flux similarly rises from ~2.4% to ~1%.

Modeling the Response of Atmospheric pCO<sub>2</sub>. We take two approaches to estimate the potential effects of an elevated Proterozoic metamorphic degassing flux on the exogenic carbon cycle (particularly atmospheric pCO<sub>2</sub> levels). The first approach considers the effects of elevated degassing on the carbon mass balance of the exogenic carbon cycle: solid-earth degassing is balanced by the chemical weathering of silicate minerals and subsequent marine carbonate burial (36–38), and the steady-state point is set by the pCO<sub>2</sub> required to generate enough silicate weathering to balance a given degassing flux (39). The second technique uses a numerical model of the Precambrian carbon cycle [PreCOSCIOUS, (40) modified to include CO<sub>2</sub> recycling by enhanced reverse weathering. Reverse weathering can be represented by the reaction

$$\begin{split} 3 & \text{Ca}^{2+}_{\text{(aq)}} + 2 \text{H}_4 \text{SiO}_{\text{4(silicic acid)}} + 6 \text{HCO}_{3\text{ (aq)}}^{-} \\ & \rightarrow \text{Ca}_3 \text{Si}_2 \text{O}_5 (\text{OH})_{\text{4(clay)}} + \text{CO}_{\text{2(fluid)}} + 5 \text{H}_2 \text{O}_{\text{(fluid)}}, \end{split} \quad \textbf{[3]} \end{split}$$

where alkalinity is consumed by clay formation and  ${\rm CO_2}$  is released. Isson & Planavsky (ref. 41) suggest that this is a potentially important feature of the Precambrian carbon cycle

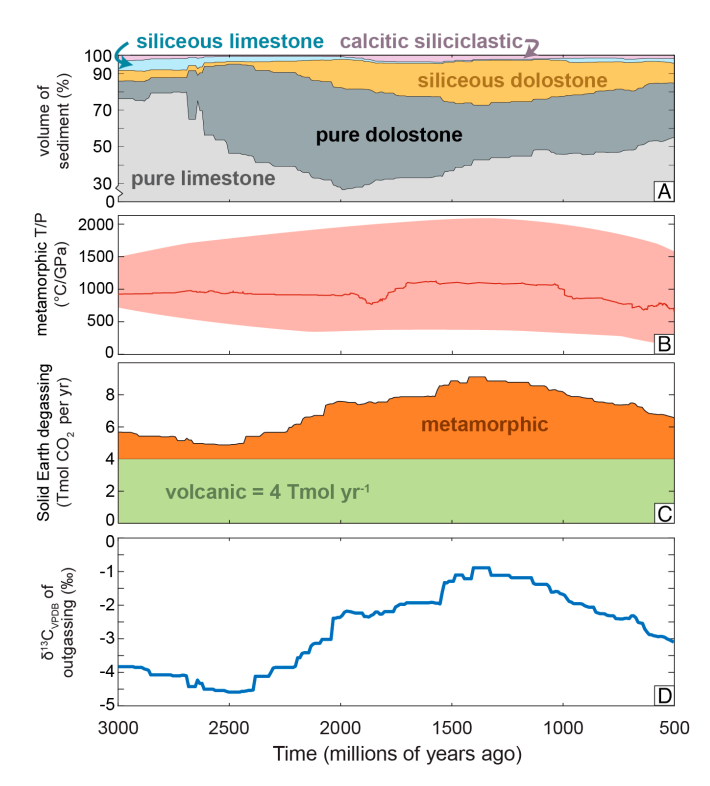


**Fig. 3.** Precambrian metamorphic decarbonation. (*A*) The volume % of each sediment type among total carbonate-bearing sediments deposited cumulatively for each time interval (data from ref. 34). (*B*) The average metamorphic T/P ratio for each time interval (after ref. 35) within the 95% prediction envelope generated by ref. 4). (*C*) The magnitude of the metamorphic carbon flux. The mean metamorphic value is shown added to a constant volcanic flux. (*D*) The carbon isotope composition of the total solid Earth degassing flux (including volcanic sources) is shown for the mean simulation.

due to elevated seawater-dissolved silica concentrations in the absence of biosilicifying organisms (e.g., ref. 42), but the extent to which reverse weathering was elevated during the Precambrian is highly uncertain, and may not have been significantly higher than modern rates (43). We therefore present modeling results with and without enhanced reverse weathering as two possible endmember scenarios.

#### Results

Phase equilibria modeling predicts a gradual rise in the metamorphic carbon flux after ~2500 Ma. Given comparable pressure—temperature conditions in the Archean and Proterozoic, this apparent rise in the metamorphic flux can primarily be attributed to changing sedimentary protolith compositions. That is, sediments deposited after ~2500 Ma were more susceptible to carbon loss when heated. The fall in metamorphic degassing after ~1400 Ma is a result of both lower T/P metamorphic conditions and dilution of dolomitic and mixed carbonate-silicate sediments with the deposition of increasingly pure limestone. We can take the Cambrian interval (541 Ma to our minimum age of 490 Ma) as representing relatively "modern" conditions. By comparison, we estimate an average total volcanic + metamorphic degassing flux near ~130% of the modern at its Mesoproterozoic peak.

How might a higher Precambrian metamorphic degassing flux affect Earth's carbon cycle and atmospheric  $pCO_2$  levels? We first consider that question in the context of the mass balance requirement for the exogenic carbon cycle: On long timescales, the sources of C to the atmosphere (including solid earth degassing) must balance the sinks (sedimentary carbon burial as carbonate

minerals and organic carbon; ref. 44). The maintenance of this balance on geologic timescales is credited to a dynamic silicate weathering flux, which removes CO2 from the atmosphere and encourages carbonate mineral precipitation and burial in sediments. The rate of silicate mineral weathering is thought to accelerate under warm (high pCO<sub>2</sub>) conditions, thus removing more CO<sub>2</sub> from the atmosphere and returning it to the solid earth as sedimentary carbonate. Under elevated solid Earth degassing, a new exogenic carbon cycle mass balance will be set at the atmospheric pCO<sub>2</sub> required to increase silicate weathering to balance the new degassing flux, which, in turn, depends on the strength of the silicate weathering feedback (e.g., ref. 39). If a mathematical form of the pCO<sub>2</sub>-silicate weathering flux relationship is assumed, then the pCO<sub>2</sub> required to balance any degassing flux can be solved analytically. A power law formulation is typically used to represent the sensitivity of silicate weathering (Fsi) to changing pCO<sub>2</sub> (e.g., refs. 39, 45, 46, and 47):

$$F_{Si} = F_{vc0} * (RCO_2)^{nSi},$$
 [4]

where  $F_{vc0}$  represents the initial degassing flux, RCO<sub>2</sub> represents the ratio of atmospheric CO2 to a reference, initial pCO2 (for example, preindustrial pCO<sub>2</sub> of 280 ppm), and nSi represents the strength of the silicate weathering feedback. This relationship can be rearranged to determine the RCO<sub>2</sub> needed to balance a higher degassing flux (i.e.,  $F_{Si}$  = a new  $F_{vc}$ ):

$$RCO_2 = (F_{vc}/F_{vc0})^{1/nSi}$$
. [5]

This relationship describes how equilibrium atmospheric pCO<sub>2</sub> responds to changing background solid Earth degassing rate, but it is very sensitive to the silicate weathering feedback strength (nSi). Because the strength of the silicate weathering feedback is uncertain and almost certainly varies significantly over the billions of years of geologic time spanned by our metamorphic degassing reconstructions (e.g., refs. 39 and 47), we consider a wide range of possible nSi values (from 0.2 to 0.6) in calculations of equilibrium atmospheric pCO<sub>2</sub> resulting from changing solid-earth degassing (Fig. 4).

The Fig. 4A illustrates the relationship between changing solid Earth degassing rate and equilibrium pCO<sub>2</sub> (Eq. 5) across a range of silicate weathering feedback strength (nSi). Our reconstructed Mesoproterozoic degassing flux (a sustained solid Earth degassing rate 30% higher than modern) would result in an equilibrium pCO<sub>2</sub> between 1.5 and 3.5 times higher than modern (median values), demonstrating the significant impact that enhanced metamorphic degassing would have on the Precambrian carbon cycle and climate.

The above framework omits a recently proposed (41) mechanism to support elevated pCO2 during the Precambrian: accelerated marine clay authigenesis ("reverse weathering") under the high seawater dissolved silica concentrations inferred for Precambrian seas in the absence of biosilicifying organisms. If marine reverse weathering was indeed much more ubiquitous during the Precambrian, this would certainly affect the relationship between elevated solid-earth degassing, silicate weathering, and atmospheric pCO<sub>2</sub>. In order to investigate the effects of enhanced metamorphic CO<sub>2</sub> release on a possible Proterozoic carbon cycle buffered by ubiquitous reverse weathering, we performed a suite of degassing rate experiments using a numerical model of the Precambrian carbon and silica cycles [PreCOSCIOUS, (40) modified to include reverse weathering (e.g., refs. 50 and 51). The sensitivity of reverse weathering rates to Precambrian seawater/pore water dissolved silica concentrations, seawater pH, temperature, and other variables is highly uncertain: Isson and Planavsky (ref. 41) explored potential

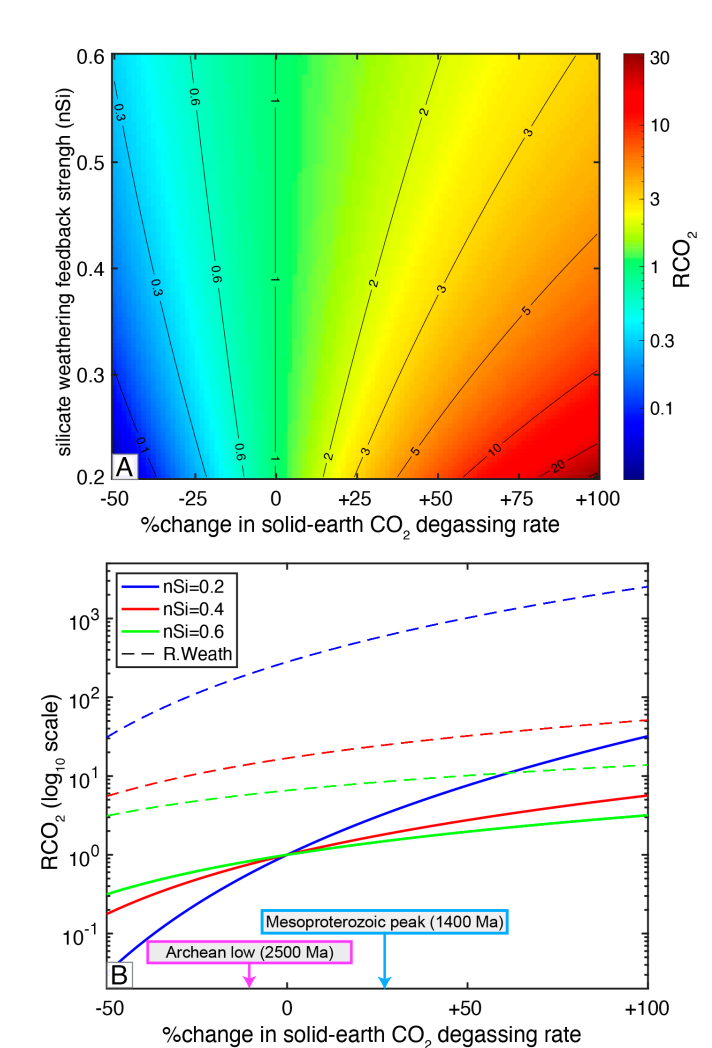
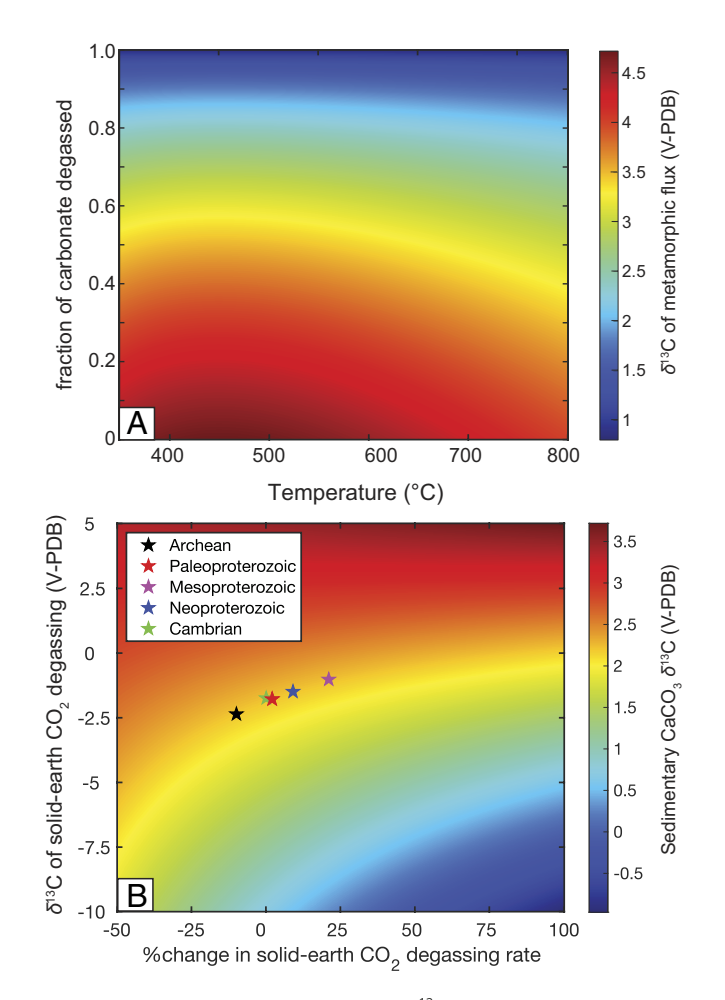


Fig. 4. Atmospheric response to elevated CO<sub>2</sub> degassing, calculated for a range of solid Earth degassing rates and silicate weathering feedback strengths. (A) Analytical solutions for equilibrium pCO<sub>2</sub> (expressed as RCO<sub>2</sub>, normalized to preindustrial CO<sub>2</sub> of 280 ppm), assuming long-term carbon cycle mass balance (Results). Note the solutions in panel a do not include reverse weathering. (B) Equilibrium  ${\sf RCO}_2$  calculated in the PreCOSCIOUS model with and without elevated reverse weathering reactions (ref. 41). Colors represent different silicate weathering feedback strengths; dashed lines include reverse weathering and solid lines omit it. Arrows indicate the percent change in solidearth CO<sub>2</sub> degassing at the lowest (Archean) and highest (Mesoproterozoic) points relative to the Cambrian period in our mean model output.

reverse weathering rates spanning orders of magnitude, concluding that elevated Precambrian dissolved silica concentrations accelerated reverse weathering rates enough to significantly affect the global carbon cycle and atmospheric pCO2 (a conclusion which has been questioned by ref. 43). For the present purposes, we parameterized reverse weathering as a function of seawater dissolved Si concentration, with a sensitivity scaled to give equilibrium atmospheric pCO<sub>2</sub> levels similar to those proposed by ref. 41. From that stable equilibrium (which already features atmospheric pCO<sub>2</sub> ~16× higher than preindustrial), the model was forced by systematically changing the total solid Earth degassing rate and then running the model for tens of millions of years until a new stable equilibrium was reached. As above, these experiments were performed under several choices of nSi (the sensitivity of the silicate weathering feedback). Because uncertainties in reverse weathering kinetics do not preclude a Precambrian carbon cycle without significantly elevated reverse weathering (43), we compare these experiments with scenarios that omit elevated reverse weathering as two possible endmembers.



**Fig. 5.** The effect of changing the rate and  $\delta^{13}C$  of solid-earth  $CO_2$  degassing on the  $\delta^{13}C$  isotopic mass balance of the exogenic carbon cycle, as recorded by sedimentary  $CaCO_3$   $\delta^{13}C$ . (*A*) the  $\delta^{13}C$  of metamorphic degassing will depend strongly upon the fraction of carbon degassed and weakly upon temperature assuming pure Rayleigh distillation. (*B*) Sedimentary  $CaCO_3$   $\delta^{13}C$  for each combination of total solid-earth degassing rate and  $\delta^{13}C$  was calculated by solving steady-state mass balance and isotopic mass balance equations describing the sources and sinks of carbon to the ocean–atmosphere system (e.g., refs. 52, 53, and 45). Silicate weathering and carbonate burial were assumed to balance changes in solid earth degassing, and for simplicity, organic carbon weathering and burial fluxes and the photosynthetic fractionation factor were fixed at modern values. Stars represent the mean value for five modeled geologic eras/periods.

The Fig. 4B shows the equilibrium atmospheric pCO<sub>2</sub> resulting from different combinations of solid-earth degassing rate and silicate weathering feedback strength in PreCOSCIOUS simulations that include accelerated reverse weathering. pCO<sub>2</sub> resulting from the same combinations of degassing rate and silicate weathering feedback strength without reverse weathering are also plotted for comparison. The absolute magnitude of atmospheric pCO<sub>2</sub> levels in simulations that include accelerated reverse weathering are of course an order of magnitude higher than modern levels, but the effect of changing solid Earth degassing rate is similar. A lower nSi (weaker silicate weathering feedback) leads to more pronounced changes in atmospheric pCO<sub>2</sub>. Simulations with degassing rates 30% higher than modern (representing the increased metamorphic CO2 production we calculate for the Mesoproterozoic) feature equilibrium pCO<sub>2</sub> levels between 1.5 and 4.1 times higher (depending on the value of nSi chosen) than those simulations run with a modern degassing rate.

The elevated rates of Proterozoic decarbonation predicted by our thermodynamic modeling would increase not just the rate of

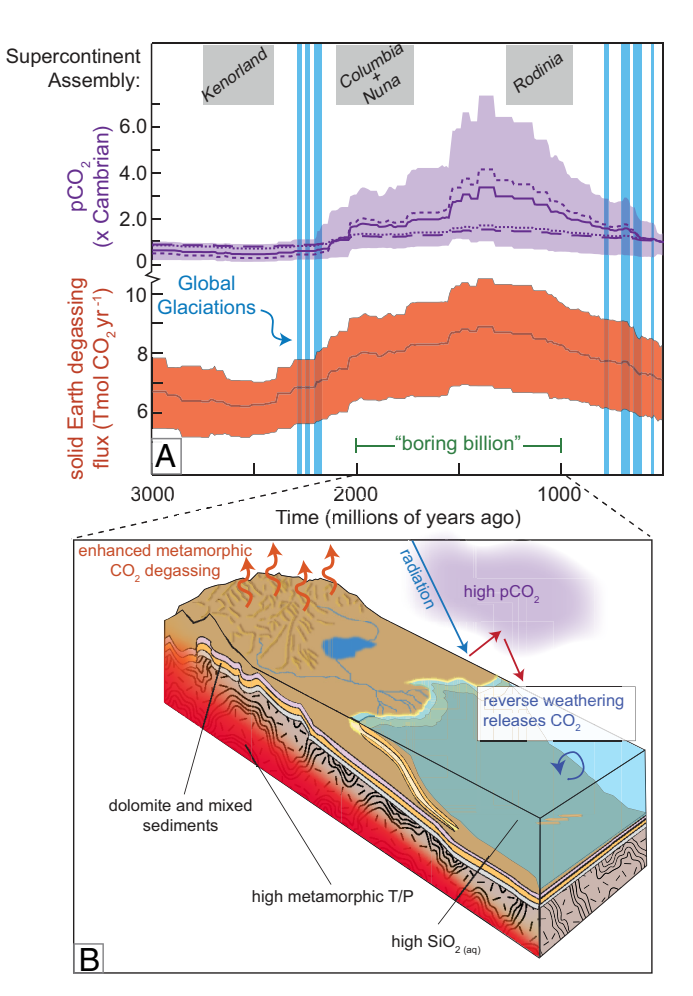


**Fig. 6.** Summary of enhanced metamorphic degassing model results. Panel A, the period between ~2000 and 1000 Ma is characterized by a higher solid Earth degassing flux (mean value and 25th to 75th percentile contours are shown). Modeled pCO $_2$  levels are shown for nSi = 0.2 without reverse weathering (short-dashed line) nSi = 0.2 with reverse weathering (solid line) nSi = 0.6 without weathering (dotted line) and nSi = 0.6 with reverse weathering (long-dash). The purple-shaded region shows the entire range of model outcomes at the 25th to 75th percentile range. Periods of elevated pCO $_2$  correspond to the "boring billion" period notably lacking global glaciations [after (48); Supercontinent assembly after (49)]. Panel B is a block diagram illustrating the proposed relationship between Proterozoic metamorphic and surface processes that may contribute to high pCO $_2$ .

total-solid earth degassing, but its  $\delta^{13}C$  as well. Total solid-earth degassing is a mixture of relatively high- $\delta^{13}C$  metamorphic CO<sub>2</sub> (~3.5‰) and lower- $\delta^{13}C$  (~5‰) mantle-derived volcanic CO<sub>2</sub>. An increase in the metamorphic component by ~1.7× (as in our average model at 1400 Ma) would drive an increase in the  $\delta^{13}C$  of degassed CO<sub>2</sub> from ~2.4‰ to ~0.9‰. We use carbon-cycle flux and isotopic mass balance calculations (45, 52, 53) to calculate what effects elevated degassing CO<sub>2</sub>  $\delta^{13}C$  would have on the exogenic carbon cycle and sedimentary  $\delta^{13}C$  records. Results of these calculations are shown in Fig. 5*B*.

The combined effects of elevated degassing rates and  $\delta^{13}C$  on sedimentary  $\delta^{13}C$  are quite small because they each independently drive opposing effects: increasing the  $\delta^{13}C$  of solid-earth degassing serves to increase the  $\delta^{13}C$  of the exogenic carbon cycle, while increasing the rate of solid-earth degassing tends to decrease the  $\delta^{13}C$  of the exogenic carbon cycle. When both are increased simultaneously, as implied by our thermodynamic modeling of Proterozoic decarbonation, the effects nearly cancel out: We calculate sedimentary  $\delta^{13}C$  values for the entire Precambrian and Cambrian within 0.1‰ of one another.

## **Discussion**

It has long been suggested that Earth's atmosphere needed higher concentrations of greenhouse gasses to maintain habitability given substantially lower solar luminosity early in our history [see the "faint young sun" problem, (54, 55); reviews in refs. 56-58]. It is, therefore, common to propose that volcanic carbon degassing may have been elevated to account for higher equilibrium pCO<sub>2</sub> (e.g., refs. 59 and 60) despite little direct evidence for enhanced volcanic CO<sub>2</sub> release on the early Earth. Additional proposed explanations include less efficient CO2 draw down via silicate weathering (e.g., ref. 41). We would by no means suggest that these processes were constant over billions of years. However, we propose that enhanced metamorphic CO<sub>2</sub> degassing offers an alternative and complementary explanation for high atmospheric pCO<sub>2</sub>, especially in the Mesoproterozoic.

Notably, our reconstructed interval of elevated metamorphic CO<sub>2</sub> release corresponds to the longest recorded period in our planet's post-Archean history devoid of global glaciation (Snowball Earth) events (e.g., refs. 61 and 62; Fig. 6). During the subsequent Neoproterozoic, the Sturtian (~715 to 660 Ma, ref. 63) and Marinoan (~635 Ma, ref. 61) "Snowball Earth" glaciations of the Cryogenian are the most extensive glaciations in Earth's history. The global-scale glaciation during these events has been attributed to a runaway ice-albedo positive feedback following the crossing of a mid-latitude polar ice cap growth threshold during a long-term cooling trend (e.g., refs. 64 and 65). The fall in metamorphic CO<sub>2</sub> degassing flux reconstructed by our thermodynamic modeling after ~1200 Ma may have contributed to this long-term cooling trend or at least cooled the background climate state of the Neoproterozoic such that secular cooling trends were more likely to cross the ice-albedo runaway threshold, triggering global glaciation.

In short, modeling suggests that metamorphic CO2 release could have dominated global carbon cycling on the Proterozoic Earth, with profound implications for the climate state, carbon isotope mass balance, and planetary habitability. Some substantial uncertainties remain—in particular, differences in the volumetric extent of metamorphism and reaction rates could modulate metamorphic CO<sub>2</sub> degassing independent of the changing decarbonation efficiency we explore here. We note that mountain-building may also be associated with enhanced silicate weathering and corresponding draw-down of atmospheric CO<sub>2</sub> (e.g., refs. 66 and 67). However, even on the modern Earth, mountain building appears to be a net source of CO<sub>2</sub> (e.g., refs. 7 and 8) emitting, perhaps, an order of magnitude more CO<sub>2</sub> than is removed (68). Thus, we consider this process a likely net source of CO2 on the earlier Earth, especially in light of evidence for enhanced metamorphic degassing.

Exactly how much enhanced degassing might have increased atmospheric pCO2 depends on the strength of the silicate weathering feedback (uncertain today, even more so for the Precambrian) and whether or not reverse weathering was supercharged to the extent that ref. 41 propose. Nevertheless, it is crucial that metamorphism be explored as a potentially major carbon source in

J. P. Grotzinger, N. P. James, Precambrian carbonates: Evolution of understanding. Soc. Sediment. Geol. Spl. Publ. 67, 3-20 (2000).

- M. Brown, Duality of thermal regimes is the distinctive characteristic of plate tectonics since the Neoarchean. Geol. 34, 961-964 (2006).
- R. M. Holder, D. R. Viete, M. Brown, T. E. Johnson, Metamorphism and the evolution of plate tectonics. Nat. 572, 378-381 (2019).
- D. M. Kerrick, K. Caldeira, Metamorphic CO<sub>2</sub> degassing from orogenic belts. Chem. Geol. 145, 213-232
- G. Chiodini et al., Quantification of deep CO2 fluxes from Central Italy. Examples of carbon balance for regional aquifers and of soil diffuse degassing. Chem. Geol. 159, 205-222 (1999).

consideration of the carbon cycle in deep time. Future work should include new field- and laboratory-based estimates of metamorphic CO<sub>2</sub> degassing. The inclusion of carbonate metamorphism in numerical models will also help define the role it played in the success of life on the early Earth.

### **Materials and Methods**

Thermodynamic Modeling of Metamorphic Decarbonation. All calculations are performed in the software package Theriak-Domino (69) with the database of ref. 70 and compatible activity models with a water-bearing fluid present in excess. Details are given in SI Appendix.

For each time interval, we calculate an average sedimentary section using rock volumes from ref. 34 and we assume all carbonate rocks of equal or older age are available for metamorphism. Dolostones and limestones "with significant silicate component" are represented by adding Marianas clay to a pure carbonate rock, while significant carbonate component in a siliciclastic rock is approximated by adding either dolomite or calcite to a pure Marianas clay. We also consider metasomatic silica addition to pure carbonate rocks in a simple system of CaO-(±MgO)-SiO<sub>2</sub>-CO<sub>2</sub>-H<sub>2</sub>O. For each time period, the carbon loss resulting from metamorphism is calculated for each protolith type at a metamorphic condition consistent with the corresponding time interval from ref. 35.

Finally, the fractional mass loss of carbon is converted to a flux according to the following equation:

$$F = \int_{z_1}^{z_2} C_{co_2} \cdot \rho \cdot \Delta CO_2 \cdot t^{-1} \cdot A \cdot dz,$$
 [6]

where  $C_{\text{CO}_2}$  is the initial mass fraction of  $\text{CO}_2$  for a given rock type,  $\rho$  is its density (fixed at 2,700 kg m<sup>-3</sup>),  $\Delta$ CO<sub>2</sub> is the fraction of carbon lost, t is the duration of metamorphism (fixed at 10 My), A is the area of metamorphism, and z is the depth of each rock type (such that  $\Delta z$  = thickness); z is estimated in the Monte Carlo simulation using a generated crustal thickness and volume fraction of carbonatebearing rock throughout the crustal stack multiplied by the proportions of each carbonate-bearing subtype according to data from ref. 34 (Fig. 3D). See similar assumptions for flux calculations in refs. 5, 9, 71, and 72.

The  $\delta^{13}C_{VPDB}$  of total degassed  $CO_2$  from each protolith along an open-system Rayleigh fractionation curve can be calculated according to

$$\delta^{13}C_{degassed} = \left[\delta^{13}C_{o}\left(F^{\alpha} - 1\right) + 1000\left(F^{\alpha} - F\right)\right] \cdot \left[F - 1\right]^{-1},$$
 [7]

where  $\delta^{13}C_0$  is the isotopic composition of the original solid, F is the fraction of carbon remaining in the rock, and  $\alpha$  is a temperature-dependent fractionation factor. The  $\delta^{13}C_0$  values are taken as +0.8% (the average for all Precambrian carbonates from ref. 73). There is no fractionation associated with degassing in carbonated siliciclastics since they undergo 100% carbon loss (i.e., quantitative removal), but the siliceous limestones and dolostones release heavily fractionated  $CO_2$  (>4.0%). The average metamorphic outgassing flux ranges from 1.1 to 2.5%.

Data, Materials, and Software Availability. All study data are included in the article and/or SI Appendix.

ACKNOWLEDGMENTS. We gratefully acknowledge funding from the NSF grant EAR- 2247049 to E.M.S. We appreciate the editorial handling at PNAS and two anonymous reviewers whose feedback substantially improved the manuscript.

- J. A. Becker, M. J. Bickle, A. Galy, T. J. Holland, Himalayan metamorphic CO<sub>2</sub> fluxes: Quantitative constraints from hydrothermal springs. Earth Planet. Sci. Lett. 265, 616-629 (2008).
- M. J. Evans, L. A. Derry, C. France-Lanord, Degassing of metamorphic carbon dioxide from the Nepal Himalaya. *Geochem. Geophys. Geosyst.* **9**, 1–18 (2008).
- A. Skelton, Flux rates for water and carbon during greenschist facies metamorphism. Geol. 39, 43-46 (2011).
- E. M. Stewart et al., Carbonation and decarbonation reactions: Implications for planetary habitability. Am. Mineral. 104, 1369-1380 (2019).
- X. Chu, C. Ť. A. Lee, R. Dasgupta, W. Cao, The contribution to exogenic CO<sub>2</sub> by contact metamorphism at continental arcs: A coupled model of fluid flux and metamorphic decarbonation. Am. J. Sci. 319,
- E. J. Ramos, J. S. Lackey, J. D. Barnes, A. A. Fulton, Remnants and rates of metamorphic decarbonation in continental arcs. GSA Today 30, 4-10 (2020).

R. E. Zeebe, P. Westbroek, A simple model for the CaCO<sub>3</sub> saturation state of the ocean: The "Strangelove", the "Neritan", and the "Cretan" Ocean. Geochem. Geophys. Geosyst. J. 4, 1-26 (2003)

- 13. T.T. Isson et al., Evolution of the global carbon cycle and climate regulation on earth. Glob. Biogeochem. Cycles. 34, 2018 006061 (2020).
- C. D. Hiett et al., Deep CO<sub>2</sub> and N<sub>2</sub> emissions from Peruvian hot springs: Stable isotopic constraints on volatile cycling in a flat-slab subduction zone. Chem. Geol. 595, 120787 (2022).
- V. M. Goldschmidt, Die Gesetze der Gesteinsmetamorphose mit Beispielen aus der Geologie des Südlichen Norwegens (The laws of rock metamorphism with examples from the geology of southern Norway) (Vi denskapsselskapets Skrifter, 1912).
- N. L. Bowen, Progressive metamorphism of siliceous limestone and dolomite. J. Geol. 48, 225-274 16.
- E. M. Stewart, J. J. Ague, Pervasive subduction zone devolatilization recycles CO<sub>2</sub> into the forearc. Nat. Commun. 11, 1–8 (2020). 17
- T. Plank, C. H. Langmuir, The chemical composition of subducting sediment and its consequences 18 for the crust and mantle. Chem. Geol. 145, 325-394 (1998).
- $A.\ B.\ Thompson,\ J.\ R.\ Ridley,\ Pressure-temperature-time\ (P-T-t)\ histories\ of\ erogenic\ belts.\ Philos.$ Trans. R. Soc. Lond. Ser. A Math. Phys. Sci. 321, 27-45 (1987).
- M. Brown, P-T-t evolution of orogenic belts and the causes of regional metamorphism. J. Geol. Soc. 150, 227-241 (1993).
- R. G. Bathurst, Carbonate Sediments and their Diagenesis (Elsevier, 1972).
- J. J. Ague, "Fluid flow in the deep crust" in Treatise on Geochemistry, H. D. Holland, K. K. Turekian, Eds. (Elsevier, 2014), pp. 203-247.
- A. J. Ridgwell, M. J. Kennedy, K. Caldeira, Carbonate deposition, climate stability, and Neoproterozoic ice ages. Sci. 302, 859-862 (2003).
- P. Hoffman, Proterozoic paleocurrents and depositional history of the East Arm fold belt, Great Slave Lake, Northwest Territories. Can. J. Earth Sci. 6, 441-462 (1969).
- J. P. Grotzinger, Evolution of Early Proterozoic passive-margin carbonate platform, rocknest fformation, wopmay orogen, Northwest Territories, Canada. J. Sediment. Res. 56, 831-847
- J. P. Grotzinger, "Facies and evolution of Precambrian carbonate depositional systems: Emergence of the modern platform archetype" in Controls on Carbonate Platforms and Basin Development, P. D. Crevello, J. L. Wilson, J. F. Sarg, J. F. Read, Eds. (SEPM, 1989), pp 44–79.
- P. G. Eriksson, O. Catuneanu, S. Sarkar, H. Tirsgaard, Patterns of sedimentation in the Precambrian. Sediment. Geol. 176, 17-42 (2005).
- A. Kriscautzky, L. C. Kah, J. K. Bartley, Molar-tooth structure as a window into the deposition and diagenesis of precambrian carbonate. Ann. Rev. Earth Planet. Sci. 50, 205-230 (2022).
- S. E. Peters, J. M. Husson, J. Wilcots, The rise and fall of stromatolites in shallow marine environments. Geol. 45, 487-490 (2017).
- R. A. Daly, First calcareous fossils and the evolution of the limestones. Bull. Geol. Soc. Am. 20, 153-170 (1909).
- A. B. Ronov, A. A. Yaroshevsky, Chemical composition of the earth's crust. Geophys. Monogr. Ser. 13, 37-57 (1969).
- 32. H. D. Holland, H. Zimmermann, The dolomite problem revisited. Int. Geol. Rev. 42, 481-490 (2000).
- J. Warren, Dolomite: Occurrence, evolution and economically important associations. Earth Sci. Rev. 33. 52, 1-81 (2000).
- $\textbf{M. D. Cantine, A. H. Knoll, K. D. Bergmann, Carbonates before skeletons: A database approach. \textit{Earth}$ Sci. Rev. 201, 103065 (2020).
- M. Brown, T. Johnson, Secular change in metamorphism and the onset of global plate tectonics. Am. Mineral. 103, 181-196 (2018).
- H. C. Urey, On the early chemical history of the earth and the origin of life. Proc. Natl. Acad. Sci U.S.A. 38, 351-363 (1952).
- 37. J. C. Walker, P. B. Hays, J. F. Kasting, A negative feedback mechanism for the long-term stabilization of Earth's surface temperature. J. Geophys. Res. Oceans 86, 9776-9782 (1981).
- R. A. Berner, A. C. Lasaga, R. M. Garrels, The carbonate-silicate geochemical cycle and its effect on atmospheric carbon dioxide over the past 100 million years. Am. J. Sci. 283, 641-683 (1983).
- D. E. Penman, J. K. C. Rugenstein, D. E. Ibarra, M. J. Winnick, Silicate weathering as a feedback and forcing in Earth's climate and carbon cycle. *Earth Sci. Rev.* **209**, 103298 (2020). D. E. Penman, A. D. Rooney, Coupled carbon and silica cycle perturbations during the Marinoan
- snowball Earth deglaciation. Geol. 47, 317-320 (2019).
- T.T. Isson, N. J. Planavsky, Reverse weathering as a long-term stabilizer of marine pH and planetary climate. Nat. 560, 471-475 (2018).
- D. J. Conley et al., Biosilicification drives a decline of dissolved Si in the oceans through geologic time. Front. Marine Sci. 4 (2017).

- 43. J. Krissansen-Totton, D. C. Catling, A coupled carbon-silicon cycle model over Earth history: Reverse weathering as a possible explanation of a warm mid-Proterozoic climate. Earth Planet. Sci. Lett. 537
- R. A. Berner, K. Caldeira, The need for mass balance and feedback in the geochemical carbon cycle. Geology 25, 995-996 (1997).
- J. C. Walker, J. F. Kasting, Effects of fuel and forest conservation on future levels of atmospheric carbon dioxide. Global Planet. Change 5, 151-189 (1992).
- R. E. Zeebe, LOSCAR: Long-term ocean-atmosphere-sediment carbon cycle reservoir model v2. 0.4. Geosci. Model Dev. 5, 149 (2012).
- J. K. Caves, A. B. Jost, K. V. Lau, K. Maher, Cenozoic carbon cycle imbalances and a variable weathering feedback. *Earth Planet. Sci. Lett.* **450**, 152–163 (2016).
- G. M. Young, Precambrian supercontinents, glaciations, atmospheric oxygenation, metazoan evolution and an impact that may have changed the second half of Earth history. Geosci. Front. 4, 247-261 (2013).
- C. J. Hawkesworth, P. A. Cawood, B. Dhuime, Tectonics and crustal evolution. Ann. Rev. Earth Planet Sci. 41, 169-198 (2016).
- F. Li et al., Reverse weathering may amplify post-Snowball atmospheric carbon dioxide levels Precambrian Res. 364, 106279 (2021).
- T. T. Isson et al., Marine siliceous ecosystem decline led to sustained anomalous Early Triassic warmth. Nat. Commun. 13, 3509 (2022).
- L. R. Kump, M. A. Arthur, Interpreting carbon-isotope excursions: Carbonates and organic matter. Chem. Geol. 161, 181-198 (1999).
- R. A. Berner, The Phanerozoic Carbon Cycle: CO and O (Oxford University Press, 2004).
- W. L. Donn, B. D. Donn, W. G. Valentine, On the early history of the earth. Geol. Soc. Am. Bull. 76, 287-306 (1965).
- C. Sagan, G. Mullen, Earth and Mars: Evolution of atmospheres and surface temperatures. Sci. 177, 52-56 (1972).
- J. F. Kasting, Faint young Sun redux. Nat. 464, 687-689 (2010).
- G. Feulner, The faint young Sun problem. *Rev. Geophys.* **50**, 1–26 (2012).
  B. Charnay, E. T. Wolf, B. Marty, F. Forget, Is the faint young Sun problem for Earth solved? *Space Sci.* 58. Rev. 216, 1-29 (2020).
- E. Tajika, Faint young Sun and the carbon cycle: Implication for the Proterozoic global glaciations. Earth Planet. Sci. Lett. 214, 443-453 (2003).
- F. Gaillard, B. Scaillet, A theoretical framework for volcanic degassing chemistry in a comparative planetology perspective and implications for planetary atmospheres. Earth Planet. Sci. Lett. 403, . 307-316 (2014).
- K. H. Hoffmann, D. J. Condon, S. A. Bowring, J. L. Crowley, U-Pb zircon year from the Neoproterozoic Ghaub Formation. Journal 32, 817-820 (2004).
- J. L. Kirschvink et al., Paleoproterozoic snowball Earth: Extreme climatic and geochemical global change and its biological consequences. Journal 97, 1400-1405 (2000).
- A. D. Rooney et al., Re-Os geochronology and coupled Os-Sr isotope constraints on the Sturtian snowball Earth. Journal 111, 51-56 (2014).
- J. L. Kirschvink, Late Proterozoic low-latitude global glaciation: The snowball earth. The Proterozoic Biosphere 52, 51-52 (1992).
- P. F. Hoffman, A. J. Kaufman, G. P. Halverson, D. P. Schrag, A neoproterozoic snowball earth. Geol. 281, 1342-1346 (1998).
- M. E. Raymo, W. F. Ruddiman, Tectonic forcing of late Cenozoic climate. Nat. 359, 117-122 (1992).
- R. G. Hilton, A. J. West, Mountains, erosion and the carbon cycle. Nat. Rev. Earth Environ. 1, 284-299
- A. Skelton, Is orogenesis a net sink or source of atmospheric CO<sub>2</sub>? Geol. Today 29, 102–107 (2013).
- C. de Capitani, K. Petrakakis, The computation of equilibrium assemblage diagrams with Theriak/ Domino software. Am. Mineral. 95, 1006-1016 (2010).
- T. J. B. Holland, R. Powell, An improved and extended internally consistent thermodynamic dataset for phases of petrological interest, involving a new equation of state for solids. J. Metamorph. Geol. 29, 333-383 (2011).
- D. M. Kerrick, K. Caldeira, Metamorphic CO<sub>2</sub> degassing and early Cenozoic paleoclimate. *GSA Today* 4.57-65 (1994).
- E. M. Stewart, J. J. Ague, Infiltration-driven metamorphism, New England, USA: Regional CO<sub>2</sub> fluxes and implications for Devonian climate and extinctions. *Earth Planet. Sci. Lett.* **489**, 123–134 (2018).
- A. Prokoph, G. A. Shields, J. Veizer, Compilation and time-series analysis of a marine carbonate δ180, 813C, 87Sr/86Sr and 834S database through Earth history. Earth Sci. Rev. 87, 113-133 (2008).